Correlations and fluctuations in high-energy nuclear collisions

Gordon Baym and B. Blättel*
Department of Physics, University of Illinois at Urbana-Champaign, 1110 West Green Street, Urbana, Illinois 61801

L. L. Frankfurt
Department of Physics, Tel Aviv University, Ramat Aviv, Israel

H. Heiselberg
NORDITA, Blegdamsvej 17, DK-2100 Copenhagen Ø, Denmark

M. Strikman
Department of Physics, Pennsylvania State University, University Park, Pennsylvania 16802
(Received 23 February 1995)

Nucleon correlations in the target and projectile nuclei are shown to reduce significantly the fluctuations in multiple nucleon-nucleon collisions, total multiplicity, and transverse energy in relativistic heavy-ion collisions, in particular for heavy projectile and target. The interplay between cross-section fluctuations, from color transparency and opacity, and nuclear correlations is calculated and found to be able to account for large fluctuations in transverse energy spectra. Numerical implementation of correlations and cross-section fluctuations in Monte Carlo codes is discussed.

PACS number(s): 25.75.+r, 11.80.La, 24.85.+p, 25.70.Mn

I. INTRODUCTION

Ultrarelativistic heavy-ion experiments at CERN and Brookhaven have provided important information on the processes involved in high-energy nucleus-nucleus collisions. Global features such as stopping, multiplicity, transverse energy, and rapidity distributions of particles can be described to a good approximation by models based on multiple hadronic collisions. However, several results in central nucleus-nucleus collisions, such as strangeness enhancement [1,2], J/Ψ enhancement [3], and large fluctuations in multiplicity and transverse-energy distributions [4,5], deviate from naive extrapolations based on summing nucleon-nucleon or nucleon-nucleus collisions. The crucial issue is to determine whether these interesting signals arise from the presence of a quark-gluon plasma or from more conventional phenomena such as rescattering and thermalization processes in the hot hadronic gas formed in the wake of the collisions. As we describe here, study of fluctuations provides a particularly valuable probe of the physics underlying these processes.

An early indication of the importance of understanding fluctuations in observables was provided by the NA34 geometrical model [4]. This model gave reasonably accurate parametrizations of the NA34 multiplicity and transverse energy (E_T) spectra in terms of summing multiple nucleon-nucleon collisions — each of which provides a distribution of transverse energy and multiplicity — with the collision geometry incorporated. However, as Baym *et al.* [5] pointed out, the fluctuations extracted in this way from experiment, as reflected in the widths of the high-energy tails of E_T distributions, are much larger than those expected from a microscopic model with the known fluctuations in transverse energy in nucleon-nucleon collisions.

We focus here on understanding the subtle and interlocking roles of the nucleon correlations in the underlying nuclear structure of the colliding nuclei, the range of the high-energy nucleon-nucleon interactions, and cross-section fluctuations in determining fluctuations in observables. In Refs. [6] and [7] we gave a brief account of the importance of including cross-section fluctuations and nuclear correlations in calculating E_T spectra. Calculations with these effects included showed that one should expect the large fluctuations apparent in the data. The present work includes a more detailed derivation of these effects.

Short-range correlations, which arise mainly from the short-range repulsion between nucleons as well as Pauli blocking, exclude other nucleons within a distance of order the correlation length, and reduce the fluctuations around the mean number $\langle N\rangle$ of nucleon-nucleon (NN) collisions that a projectile makes while traversing the target nucleus. For example, a high-energy proton making a central collision with a heavy nucleus, e.g., ^{208}Pb, interacts on average with $\langle N\rangle = 2\sigma\rho_0 R \simeq 7$ target nucleons. The interaction zone is small compared to the volume of the nucleus but large compared to that of a single nucleon. For a target nucleus containing an uncorrelated gas of nucleons freely running about, the number of target nucleons in the interaction zone can range from none to all, as given by the binomial distribution, leading to large flucutations in N. However, the nuclear matter in the nucleus is in fact a strongly correlated self-bound liquid, not a gas; the density fluctuations are shorter ranged, and the fluctuations in the number of nucleons in the interaction zone greatly reduced. This effect is even more significant for nucleus-nucleus collisions.

Since the correlation length is of order the internucleon distance, itself of order the range of the interactions or the

*Current address: SAP AG, Neurott str. 16, D-69190 Walldorf, Germany.

cross-sectional distance $r_s \equiv (\sigma/\pi)^{1/2}$, fluctuations in observables depend as well on the detailed interplay of the correlations and the range of the interactions. A normal assumption in microscopic models is that the projectile interacts with all nucleons in the tube along its trajectory with area given by the total NN cross section. However, allowing a more diffuse interaction range tends to reduce the importance of correlations, and to increase the fluctuations, as will become evident below.

We primarily develop the study of correlations and fluctuations within the framework of binary collisions of target and projectile nucleons, but we briefly look as well at the predictions of the "wounded-nucleon" description of sources in terms of participant nucleons. The underlying basis of the binary-collision picture is the cutting rules in the field-theoretic diagrammatic analysis of high-energy scattering processes that were found by Abramovskiĭ, Gribov, and Kancheli (AGK) [8] and Bertocchi and Treleani [9] within the inelastic eikonal approximation. These rules imply exact cancellations between inelastic interactions of the projectile with more than one nucleon at a time. They thus imply that in nucleon-nucleus scattering, away from the projectile fragmentation region, inclusive particle production is that in NN scattering times the number of nucleons, A, in the target nucleus; in nucleus-nucleus (BA) scattering away from the nuclear fragmentation regions, the result is that in NN scattering times BA, the numbers of nucleons in the projectile and target. In the fragmentation regions, shadowing effects must also be taken into account. In the Appendix we discuss the kinematical regions where the AGK theorem is valid; we also indicate how one can establish the correspondence between the basic probabilistic formulas deduced in this paper from geometrical arguments and the field-theoretic combinatorics of the AGK approach.[1]

Although we describe the initial stage of a nucleus-nucleus collision in terms of nucleonic degrees of freedom, the internal quark-gluon degrees of freedom of the colliding nucleons play an increasingly important role at higher energies. These are properly accounted for by including nucleon-nucleon cross-section fluctuations in the description of the initial collision. The basic picture is that, owing to freezing of quark-gluon color configurations in the projectile from Lorentz slowing down, the probability of a given cross section σ in a primary collision is given by a distribution function $P(\sigma)$, instead of the cross section always taking a constant (mean) value. Cross-section fluctuations increase the fluctuations in the number of collisions, as shown in [6].

In Ref. [14] we discussed in detail the nature of cross-section fluctuations in nucleon-nucleon interactions, and those of pion-nucleon interactions in Ref. [15], and showed how the distribution function P for cross-section fluctuations can be determined from both inelastic shadowing in nucleon-deuteron scattering, and from diffractive excitation in high-energy nucleon-nucleon scattering. In the Appendix we briefly discuss cross-section fluctuations within the AGK framework. To determine color fluctuations at RHIC energies we may use ISR data for diffractive processes in NN scattering [12]. At very high energies, e.g., at LHC, when a sufficiently large number of quark-gluon configurations are frozen during collisions, the parton wave function of a fast nucleus becomes different from that for a nucleus considered as a gas of interacting nucleons. In particular, nuclear shadowing effects strongly modify the small x component of the nucleus parton wave function [13]. The theoretical description of color fluctuation effects in AA collisions in this regime thus requires further elaboration. We do not address this problem here, nor the dynamics of possible violation of probabilistic picture. We also do not discuss effects of long range correlations in space that possibly arise from the interactions of produced particles with each other.

This paper is organized as follows. In Sec. II we first calculate the effect of nuclear correlations on fluctuations in the number of multiple NN interactions in proton-nucleus collisions. We then generalize the results to nucleus-nucleus collisions in Sec. III. In the Sec. IV we extend the analysis to include contributions from cross-section fluctuations, and then in Sec. V we apply these results to the question of the fluctuations in the tails of multiplicity and transverse energy distributions. In the final section we summarize and outline the procedure necessary to implement the effects discussed here in the Monte Carlo descriptions of AA collisions, and in the Appendix discuss the AGK theorem.

II. CORRELATIONS AND FLUCTUATIONS IN PROTON-NUCLEUS COLLISIONS

To gain a first understanding of the effect of nuclear correlations on fluctuations, we begin by examining collisions of protons with heavy nuclei, and treat the more complicated case of nucleus-nucleus collisions below. Neglecting cross-section fluctuations at this point, we take the NN inelastic cross section to be its average value, $\sigma = \bar{\sigma} \simeq 32$ mb (at CERN energies).

The mean number of nucleon-nucleon collisions, N, that a proton at impact parameter $\mathbf{b}$ makes with the target nucleus can be written, in the impact parameter formalism of Ref. [16], as

$$\langle N \rangle = \int d^3 r \rho_A(r) \frac{d\sigma}{d^2 b}(\mathbf{b} - \mathbf{r}_\perp), \tag{1}$$

where ρ_A is the nuclear density distribution, $\mathbf{r}_\perp$ is the transverse coordinate, and $(d\sigma/d^2 b)(\mathbf{b} - \mathbf{r}_\perp)$ is the probability for the projectile nucleon with impact parameter $\mathbf{b}$ to collide

[1] The experimental situation does not make a clear case for either an underlying binary-collision or wounded-nucleon description. In addition to the elementary collision processes described by the AGK theorem, experiments are sensitive to secondary interactions (rescattering) as well as coherent processes, e.g., showers of particles overlapping spatially and interacting strongly, which the binary picture does not account for. Proportionality of the inclusive spectrum to A at midrapidities is observed experimentally, e.g., in the recent systematic study by Whitmore *et al.* of pA scattering at 100 and 320 GeV lab energy [10]. The faster than $\sim A$ dependence for low total momentum secondary hadrons observed near the nuclear fragmentation regime is likely due to secondary hadron interactions, including interaction of produced hadrons with residual nucleons. On the other hand, experimental ^{16}O+Em(ulsion) data [11] indicate that total multiplicity is intermediate to that of the binary-collision model and the wounded-nucleon model.

with a target nucleon at position $\mathbf{r}$. In the eikonal approximation[2] with straightline geometry for multiple NN collisions — the Glauber approximation — $d\sigma/d^2b$ depends only on the transverse coordinates $\mathbf{r}_\perp$; it has an interaction range $\sim r_s \simeq 1$ fm and obeys the sum rule

$$\int d^2r_\perp \frac{d\sigma}{d^2b}(\mathbf{r}_\perp)=\sigma. \tag{2}$$

As we shall see below, it is important to take the range of the interaction into account in the multiple NN scattering problem since it is comparable to the average internucleon distance $r_0=(3/4\pi\rho_0)^{1/3}\simeq 1.16$ fm (where $\rho_0\simeq 0.16$ fm^{-3} is nuclear matter density), as well as the correlation length ξ between nucleons in a nucleus, $\simeq 1$ fm. Since $r_s \ll R_A$ (the target radius) the mean number of NN interactions can, aside from a small correction at the nuclear surface, be calculated without detailed knowledge of $d\sigma/d^2b$; using (2) we have

$$\langle N\rangle=\sigma\int_{-\infty}^{\infty} dz\rho_A(\mathbf{b},z)\equiv\sigma T_A(\mathbf{b}), \tag{3}$$

where $T_A(\mathbf{b})$ is the thickness function for the target nucleus with mass number A. If the nucleus is assumed to have constant density ρ_0 with radius $R_A=r_0A^{1/3}$, then $T_A(b)=2\rho_0(R_A^2-b^2)^{1/2}$.

The fluctuation in the number of collisions, N, at impact parameter $\mathbf{b}$, is similarly given by[3]

$$\langle N(N-1)\rangle=\int d^3rd^3r'\rho_A^{(2)}(\mathbf{r},\mathbf{r}')\frac{d\sigma}{d^2b}(\mathbf{b}-\mathbf{r}_\perp)\frac{d\sigma}{d^2b}(\mathbf{b}-\mathbf{r}'_\perp). \tag{4}$$

Here $\rho_A^{(2)}$ is the two-body density distribution

$$\rho_A^{(2)}(\mathbf{r},\mathbf{r}')=\langle\psi^\dagger(\mathbf{r})\psi^\dagger(\mathbf{r}')\psi(\mathbf{r}')\psi(\mathbf{r})\rangle \equiv\rho_A(r)\rho_A(r')[1-C_A(\mathbf{r},\mathbf{r}')], \tag{5}$$

where $\psi^\dagger$ and ψ are the nucleon creation and annihilation operators. Because nucleons tend to stay away from each other at short distances, each nucleon is surrounded by a *correlation hole*, described by the correlation function $C_A(\mathbf{r},\mathbf{r}')$, which generally, as a function of $\mathbf{r}'$, is nonvanishing about the nucleon at $\mathbf{r}$ over a range ξ in $|\mathbf{r}-\mathbf{r}'|$ of order 1 fm in nuclear matter. From the commutation relations of ψ and $\psi^\dagger$ one readily derives the sum rule on the correlation hole

$$\int d^3r'\rho_A(r')C_A(\mathbf{r},\mathbf{r}')=1, \tag{6}$$

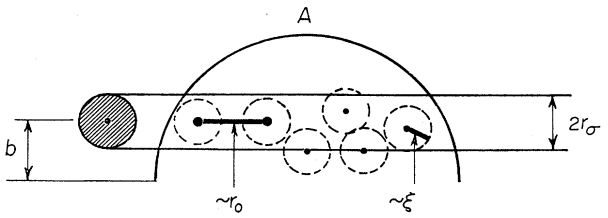

FIG. 1. Straight-line geometry of a proton-nucleus collision displaying the length scales of the cross-sectional distance r_s, the interparticle spacing r_0, and the correlation length ξ.

which says that the hole depletes precisely one nucleon. Equation (5) implies that $C_A\leq 1$. For a nuclear liquid, one expects C_A to be non-negative, as is borne out by detailed calculations [17].[4]

With (5), we can write (4) as

$$\langle N(N-1)\rangle=\int d^3rd^3r'\rho_A(r)\rho_A(r')[1-C_A(\mathbf{r},\mathbf{r}')] \times\frac{d\sigma}{d^2b}(\mathbf{b}-\mathbf{r}_\perp)\frac{d\sigma}{d^2b}(\mathbf{b}-\mathbf{r}'_\perp)\equiv(\langle N\rangle^2-\langle N\rangle\alpha), \tag{7}$$

where we define the dimensionless parameter α by

$$\alpha=\langle N\rangle^{-1}\int d^3\mathbf{r}\,d^3\mathbf{r}'\rho_A(r)\rho_A(r')C_A(\mathbf{r};\mathbf{r}') \times\frac{d\sigma}{d^2b}(\mathbf{b}-\mathbf{r}_\perp)\frac{d\sigma}{d^2b}(\mathbf{b}-\mathbf{r}'_\perp). \tag{8}$$

Physically, the parameter α measures the fraction of the overlap between the collision volume and the volume of the correlation hole described by C_A (Fig. 1). To see this let us take the correlation function to be spherically symmetric, i.e., $C_A(\mathbf{r},\mathbf{r}')=C_A(|\mathbf{r}-\mathbf{r}'|)$. Noting that for large nuclei both r_s and ξ are much smaller than the nuclear radius, and for nonperipheral collisions the integral in (8) is dominated by the bulk of the nucleus and is independent of impact parameter, we see that Eq. (8) reduces to

$$\alpha=\frac{\rho_0}{\sigma}\int dzd^2r_\perp d^2r'_\perp C_A(\sqrt{z^2+(\mathbf{r}_\perp-\mathbf{r}'_\perp)^2}) \times\frac{d\sigma}{d^2b}(\mathbf{r}_\perp)\frac{d\sigma}{d^2b}(\mathbf{r}'_\perp)\ . \tag{9}$$

From Eq. (7) we obtain the variance in the number of collisions,

[2]By eikonal here we mean that projectile nucleons are only allowed to scatter on target nucleons and visa versa.

[3]In writing (4) we neglect Glauber shadowing in the interaction of the projectile with several nucleons of the nucleus. As discussed in the Appendix, AGK cancellation [8,9] in the Glauber model justifies this neglect when calculating average characteristics of the final state away from the projectile fragmentation region.

[4]One can imagine situations in which C_A could be negative, e.g., halo nuclei (^{11}Li) or helium clustering inside light nuclei. In these systems high density "lumps" inside the nucleus increase the density fluctuations tending to make C_A negative at small separations. However, such effects are overwhelmed by short range correlations.

$$\omega_N \equiv \frac{\langle N^2\rangle - \langle N\rangle^2}{\langle N\rangle} = 1-\alpha \ . \tag{10}$$

This equation shows that nuclear correlations, through the quantity α, reduce the fluctuations in proton-nucleus collisions; we shall see below that nucleus-nucleus collisions are even more sensitive to nuclear correlations. The parameter α varies from zero, for an uncorrelated gas of nucleons, to unity, for a strongly correlated system, independent of the detailed forms of the correlation and collision probability functions. It is instructive first to evaluate α in various limits, and then consider the general case.

A. Extreme optical limit

In the extreme optical limit in which the range of the interation r_s is negligible, i.e., $r_s \ll \xi$, the NN scattering probability $d\sigma/d^2b$ can be approximated by

$$\frac{d\sigma}{d^2b}(\mathbf{b}-\mathbf{r}_\perp) \simeq \sigma\delta^{(2)}(\mathbf{b}-\mathbf{r}_\perp) \ . \tag{11}$$

Then from Eq. (9) we find that

$$\alpha \simeq \sigma\rho_0 \int dz C_A(z) \ , \quad r_s \ll \xi. \tag{12}$$

The parameter α can thus be interpreted as the *optical depth* of the correlation hole, the width in nucleon mean-free paths, $1/\sigma\rho_A$, across the hole.

If the correlation function is a simple step function, $C_A(|\mathbf{r}-\mathbf{r}'|) = \Theta(\xi - |\mathbf{r}-\mathbf{r}'|)$, then the sum rule (6) implies that $\xi = r_0 = (3/4\pi\rho_0)^{1/3}$, and we obtain

$$\alpha \simeq \frac{3}{2}\frac{\sigma}{\pi\xi^2} \ , \quad r_s \ll \xi. \tag{13}$$

B. Ideal gas

In an ideal gas with A distinguishable particles, the correlation function is a constant $C_A = 1/A$ determined by the sum rule; the correlation "hole" extends without structure across the entire nucleus (see Fig. 2). In this case we can also use Eq. (11) and find from Eq. (8) that for collisions at small impact parameter,

$$\alpha = \langle N\rangle/A \ , \tag{14}$$

which coincides with the result (13) for $\xi = R$. The term $1-\alpha$ in Eq. (10) is then the standard binomial result for the fluctuations in the number of collisions of a projectile passing through an uncorrelated nuclear gas, with individual collision probability $p = \langle N\rangle/A = \alpha$. This is the minimum value for α, corresponding to maximum fluctuations, and correlation length ξ of order the nuclear radius.

C. Maximum correlations

When $\xi \ll r_s$ we can write

$$\rho_A(r) C_A(\mathbf{r},\mathbf{r}') \simeq \delta^{(3)}(\mathbf{r}-\mathbf{r}') \ , \tag{15}$$

and find from Eq. (8) that

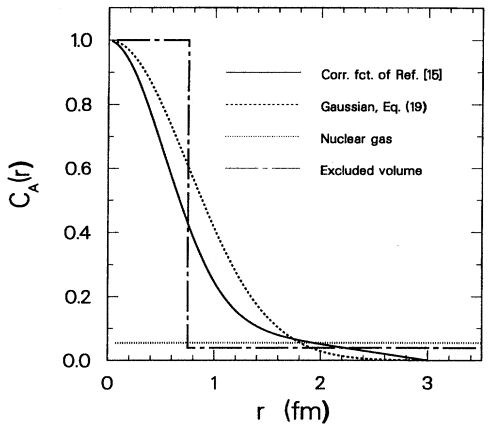

FIG. 2. Correlation functions from [17] (solid curve), the Gaussian fit, Eq. (19) (short-dash curve), an ideal gas, $C_A = 1/A$ (dotted curve), and a gas with excluded volume (long-dash curve) for a nucleus with $A = 208$.

$$\alpha = \frac{1}{\sigma}\int d^2b \left(\frac{d\sigma}{d^2b}(\mathbf{b})\right)^2 \ , \quad \xi \ll r_s \ . \tag{16}$$

If we assume, as one often does in event generators simulating multiple NN collisions, that the projectile nucleon collides with all nucleons situated within a tube of cross-sectional area σ along the beam axis with impact parameter $\mathbf{b}$ (see Fig. 1), i.e.,

$$\frac{d\sigma}{d^2b}(\mathbf{b}-\mathbf{r}_\perp) = \Theta(r_s - |\mathbf{b}-\mathbf{r}_\perp|) \ , \tag{17}$$

we find

$$\alpha = 1 \ , \quad \xi \ll r_s \ , \tag{18}$$

the maximum value of α. As Eq. (10) shows, the fluctuations in the number of binary collisions vanishes in this case. This result is due to the fact that in this limit each nucleon is confined to its correlation hole, and for $\xi \ll r_s$ the number of nucleons within the tube is determined by the ratio of the volume of the tube to the volume of the correlation hole and cannot fluctuate around that value.

D. Gas with excluded volume

In event generators, nucleon correlations are as a rule approximated by not allowing two nucleons to be situated within a distance $\tilde{\xi}$ of each other. The correlation function becomes in this way that of a gas with an excluded volume (see Fig. 2), which to a first approximation, when $\tilde{\xi} \leq r_0$, is given by $C_A = 1$ for $r \leq \tilde{\xi}$ and, from the sum rule, $C_A = (r_0^3 - \tilde{\xi}^3)/R_A^3$ for $r > \tilde{\xi}$. Since α is linearly proportional to the correlation function, it is the weighted sum of the two pieces. To evaluate the first term, we use Eq. (18) when $\tilde{\xi} \ll r_s$, and Eq. (12) when $\tilde{\xi} \gg r_s$; for the second term we use Eq. (14) generally, and find in the two extreme limits,

$$\alpha=\begin{cases}\dfrac{\tilde{\xi}^3}{r_0^3}+\left(1-\dfrac{\tilde{\xi}^3}{r_0^3}\right)\dfrac{\langle N\rangle}{A}, & \tilde{\xi}\ll r_s\\ \dfrac{3}{2}\dfrac{\sigma\tilde{\xi}}{\pi r_0^3}+\left(1-\dfrac{\tilde{\xi}^3}{r_0^3}\right)\dfrac{\langle N\rangle}{A}, & \tilde{\xi}\gg r_s .\end{cases}$$

A numerical calculation for general $\tilde{\xi}/r_s$ with the "tube" cross-sectional area of Eq. (17) results in fluctuations well approximated by the first line of this equation, except for larger values of $\tilde{\xi}$, where α is reduced by approximately 20%. It is important to note that the fluctuations and α are very sensitive to the choice of $\tilde{\xi}$. In the following section we treat more generally the situation where the range of the correlation function is comparable to r_s.

E. General case

The nucleus is a saturated self-bound liquid and is thus strongly correlated, as can be seen from the correlation function of Fig. 2 taken from Ref. [17]. Since the correlation length ξ is of order the internucleon distance $r_0=(3/4\pi\rho_0)^{1/3}\simeq 1.17$ fm, itself of order $r_s\simeq 1.0$ fm, α depends on the detailed structure of C_A and $d\sigma/d^2b$. To make the discussion of the general situation more specific, we construct simple parametrizations of both the correlation function and the scattering probability, $d\sigma/d^2b$. In particular we assume a Gaussian form for the correlation function (see Fig. 2),

$$C_A(\mathbf{r},\mathbf{r}')=e^{-(\mathbf{r}-\mathbf{r}')^2/2\xi^2} . \tag{19}$$

The sum rule (6) relates the correlation length ξ to the nuclear density by

$$\xi=r_0(2/9\pi)^{1/6}\simeq 0.75 \text{ fm} . \tag{20}$$

[The results here can easily be generalized to a correlation function consisting a sum of several Gaussians, which more closely fits calculated correlation functions, e.g., in Ref. [17]. See Fig. 2.]

In the impact parameter formalism of Ref. [16], the imaginary part of the scattering amplitude, $\mathrm{Im}\, f(q)$, for momentum transfer q, is related to the collision probability function by

$$\mathrm{Im}f(q)=\frac{k}{4\pi}\int d^2b e^{i\mathbf{q}\cdot\mathbf{b}}\frac{d\sigma}{d^2b}(\mathbf{b}) , \tag{21}$$

where k is the incident momentum. Note that as $q\to 0$, Eq. (21) yields the optical theorem,

$$\sigma=\frac{4\pi}{k}\mathrm{Im}f(q=0) . \tag{22}$$

At high energies, the imaginary part of the scattering amplitude can be parametrized as

$$\mathrm{Im}f(q)=\frac{k\sigma}{4\pi}e^{-q^2r_\sigma^2/4} . \tag{23}$$

The slope parameter r_σ^2 depends weakly on energy, and at CERN energies, $E_{\text{lab}}\simeq 200$ GeV, $r_\sigma\simeq 1.2$ fm [16]. With this form we find

$$\frac{d\sigma}{d^2b}(\mathbf{b})=\frac{\sigma}{\pi r_\sigma^2}e^{-b^2/r_\sigma^2} . \tag{24}$$

Substituting the two Gaussian parametrizations, (19) and (24) in the definition of α, Eq. (8), and making use of the fact that both ξ and r_s are $\ll R$, we find

$$\alpha=\frac{\rho_0\sigma}{(\pi r_\sigma^2)^2}\int dz\, e^{-z^2/2\xi^2}\int d^2r_\perp d^2r'_\perp\, e^{-(\mathbf{r}_\perp-\mathbf{r}'_\perp)^2/2\xi^2}\times e^{-(r_\perp^2+r_\perp'^2)/r_\sigma^2}, \tag{25}$$

which, by transforming to coordinates $\mathbf{r}_\perp\pm\mathbf{r}'_\perp$, and using the relation (20) is readily evaluated as

$$\alpha=\frac{1}{2\pi}\frac{\sigma}{\xi^2+r_\sigma^2} . \tag{26}$$

In order that the collision probability function, (24), be less than unity, the condition $\sigma\leq\pi r_\sigma^2$ or equivalently $r_s\leq r_\sigma$ must be satisfied. [Note that $r_s=(\sigma/\pi)^{1/2}$ determines the strength of the interaction whereas r_σ determines its range.] For the values for r_σ and σ quoted above $\sigma\leq\pi r_\sigma^2$ is indeed satisfied. This condition, used in (26), implies that $\alpha\leq 1/2$. This surprising result does not in fact disagree with the earlier result $\alpha=1$ in (18) since there $d\sigma/d^2b$ was assumed to be a step function. Employing a diffuse form for $d\sigma/d^2b$ has the physical consequence that two nucleons lying on the same projectile trajectory are not necessarily both hit, which softens the restrictions from the correlations of the nucleons and results in a smaller value of α. With the actual values $\xi=0.75$ fm, $r_\sigma=1.2$ fm and $\sigma=32$ mb given above, we find $\alpha=0.25$.

F. Numerical studies

Pieper [18] has calculated the detailed probability distribution $P_N(b)$ for a proton colliding with various closed-shell nuclei numerically using correlated many-body wave functions, with the assumption that $d\sigma/d^2b$ is given by the step function of Eq. (17). The distribution function is considerably narrower for central collisions than a Poisson. By counting the number of nucleons in cylinders of radius 1 fm (corresponding to $\sigma=32$ mb) he finds, for central events, $\alpha\simeq 0.31-0.33$ for both small ($A=40$) and large systems ($A=224$). In addition, the fluctuations are found to increase towards unity (corresponding to vanishing α) for peripheral events. (Taking only the correlations of a free Fermi gas of neutrons and protons into account yields $\alpha=0.25$ for central collisions.) Pieper's value for α is larger than found above, $\alpha=0.25$, primarily because of his use of a step-function form for $d\sigma/d^2b$ instead of a more diffuse Gaussian.

III. FLUCTUATIONS IN NUCLEUS-NUCLEUS COLLISIONS

We now generalize the calculation of the number of NN collisions and its fluctuations to nucleus-nucleus collisions. We continue to assume the Glauber approximation with straight line geometry; the assumption that the nucleons do not move between successive hits is valid at high energies as a consequence of Lorentz contraction of the nuclei and the relatively small transverse momentum transfers in NN collisions.

The mean number of NN collisions in a central ($\mathbf{b}=0$) collision of a projectile nucleus B with a target nucleus A is given by

$$\langle N\rangle = \int d^3r\,d^3r'\,\rho_B(r)\rho_A(r')\frac{d\sigma}{d^2b}(\mathbf{r}_\perp-\mathbf{r}'_\perp)$$
$$\simeq\sigma\int dz\,dz'\,d^2s\,\rho_B(\mathbf{s},z)\rho_A(\mathbf{s},z')=\sigma\int d^2s\,T_B(s)T_A(s), \tag{27}$$

where we assume $\sigma\ll R_B^2, R_A^2$. When the projectile is small, i.e., $R_B^2\ll R_A^2$, the mean number of collisions becomes

$$\langle N\rangle\simeq B\sigma\rho_0 R_A, \quad B\ll A\ , \tag{28}$$

which is just B times the number of NN collisions in a central proton-nucleus collision.

The fluctuations in the number of NN collisions are found from

$$\langle N^2\rangle=\langle N\rangle+\int d^3r\,d^3r''\,d^3r'''\,\rho_B(r)\rho_A^{(2)}(\mathbf{r}'',\mathbf{r}''')\frac{d\sigma}{d^2b}(\mathbf{r}_\perp-\mathbf{r}''_\perp)\frac{d\sigma}{d^2b}(\mathbf{r}_\perp-\mathbf{r}'''_\perp)+\int d^3r\,d^3r'\,d^3r''\,\rho_B^{(2)}$$
$$\times(\mathbf{r},\mathbf{r}')\rho_A(r'')\frac{d\sigma}{d^2b}(\mathbf{r}_\perp-\mathbf{r}''_\perp)\frac{d\sigma}{d^2b}(\mathbf{r}'_\perp-\mathbf{r}''_\perp)+\int d^3r\,d^3r'\,d^3r''\,d^3r'''\,\rho_B^{(2)}(\mathbf{r},\mathbf{r}')\rho_A^{(2)}(\mathbf{r}'',\mathbf{r}''')\frac{d\sigma}{d^2b}(\mathbf{r}_\perp-\mathbf{r}''_\perp)\frac{d\sigma}{d^2b}(\mathbf{r}'_\perp-\mathbf{r}'''_\perp). \tag{29}$$

The four terms in Eq. (29) correspond to: (i) the same projectile nucleon colliding with the same target nucleon, (ii) the same projectile at position $\mathbf{r}$ colliding with two different nucleons at positions $\mathbf{r}''$ and $\mathbf{r}'''$ in the target, (iii) a nucleon at $\mathbf{r}''$ in the target being hit by the two different nucleons at $\mathbf{r}$ and $\mathbf{r}'$ in the projectile nucleus, and finally, (iv) two different nucleons at positions $\mathbf{r}$ and $\mathbf{r}'$ in the projectile nucleus colliding with two different nucleons at positions $\mathbf{r}''$ and $\mathbf{r}'''$ in the target nucleus.

The second term in (29) is evaluated analogously to the proton-nucleus case and is

$$=\sigma\int d^2s\,T_B(s)T_A^2(s)\ -\langle N\rangle\alpha, \tag{30}$$

while the third term in (29) contains the two-body density distribution of nucleus B and gives a contribution

$$=\sigma\int d^2s\,T_B^2(s)T_A(s)\ -\langle N\rangle\beta, \tag{31}$$

where $\beta\simeq\alpha$ is the correlation parameter for nucleus B, defined analogously to Eq. (8).

The fourth term in Eq. (29) reduces to

$$\langle N\rangle^2-\sigma\int d^2\mathbf{s}\,T_B(s)T_A^2(s)-\sigma\int d^2\mathbf{s}\,T_B^2(s)T_A(s)+\gamma\langle N\rangle\ . \tag{32}$$

The four terms here arise from each nuclear two-body density distribution having two terms [cf. (5)]; they correspond respectively to the product (i) without any nuclear correlation functions, (ii) with one correlation function from nucleus A, (iii) with one correlation function for nucleus B, and finally (iv) the product containing both correlation functions. The first three terms in (32), which contain only one or no nuclear correlation function, are straightforward to calculate and do not depend on the detailed forms of the correlation functions or the collision probability function, as long as ξ and r_σ are much smaller than the nuclear radii. The last term is more tedious to evaluate because it contains the products of both correlation functions and two collision probabilities; these enter in the parameter γ defined by

$$\gamma=\langle N\rangle^{-1}\int d^3r\,d^3r'\,d^3r''\,d^3r'''\ \rho_B(r)\rho_B(r')\rho_A(r'')\rho_A(r''')$$
$$\times C_B(\mathbf{r}-\mathbf{r}')C_A(\mathbf{r}''-\mathbf{r}''')\frac{d\sigma}{d^2b}(\mathbf{r}_\perp-\mathbf{r}''_\perp)\frac{d\sigma}{d^2b}(\mathbf{r}'_\perp-\mathbf{r}'''_\perp)\ . \tag{33}$$

With the Gaussian forms for the correlation function, Eq. (19), and for the scattering probability, Eq. (24), we find

$$\gamma=\frac{1}{2\pi}\frac{\sigma}{r_\sigma^2+2\xi^2}=\alpha\frac{r_\sigma^2+\xi^2}{r_\sigma^2+2\xi^2}\ . \tag{34}$$

The variance in the number of binary collisions, found from Eqs. (29)–(32), is

$$\omega_N=1+\gamma-\alpha-\beta. \tag{35}$$

This result generalizes the proton-nucleus result, Eq. (10), to nucleus-nucleus collisions, and improves the result derived in [6] which assumed $\gamma=1$. With $\xi=0.75$, $r_\sigma=1.2$ fm, and $\sigma=32$ mb we find $\alpha=\beta=0.25$, $\gamma=0.15$, and $\omega_N=0.65$.

The derivation of Eq. (35) assumes that the correlation length ξ is much smaller than the nuclear radii, R_B and R_A, as is the case for a strongly correlated nuclear fluid.[5] The importance of including the correct correlations is well-illustrated by calculating the fluctuations in the opposite limit in which the nucleons are allowed to swarm around in the nucleus as a free gas. The correlation functions are then $C_A=1/A$ and $C_B=1/B$, and when $r_\sigma \ll R_B \ll R_A$, one obtains directly from (29) that

$$\langle N^2\rangle = \langle N\rangle + \sigma^2 \int d^2s T_B(s) T_A^2(s)\left(1-\frac{1}{A}\right) + \sigma^2 \int d^2s T_B^2(s) T_A(s)\left(1-\frac{1}{B}\right) + \langle N\rangle^2\left(1-\frac{1}{A}\right)\left(1-\frac{1}{B}\right), \quad (36)$$

where the terms correspond to the successive terms in (29). The resulting expression for the variance follows from Eqs. (29) and (36):

$$\omega_N = 1-\frac{B}{A}N_{pA}+\frac{B-1}{B}N_{pB} \quad \text{(nuclear gas)}, \quad (37)$$

where we define

$$N_{pA}=\langle N\rangle^{-1}\sigma^2\int d^2s T_B(s)T_A^2(s), \quad (38)$$

$$N_{pB}=\langle N\rangle^{-1}\sigma^2\int d^2s T_B^2(s)T_A(s). \quad (39)$$

The quantities N_{pA} and N_{pB} are straightforward to calculate for small projectiles, since then $T_A(s)\simeq 2\rho_0 R_A$; N_{pA} reduces to the number of NN collisions in central proton-nucleus collisions,

$$N_{pA}\simeq 2\sigma\rho_0 R_A, \quad B\ll A, \quad (40)$$

and

$$N_{pB}\simeq \tfrac{3}{2}\sigma\rho_0 R_B, \quad B\ll A. \quad (41)$$

The factor 3/2 instead of 2 follows from the impact parameter averaging necessary for the projectile nucleus in the limit $B\ll A$.

To calculate N_{pA} and N_{pB} more generally, we first assume uniform density nuclei with sharp surfaces. Then from (1) we find,

$$\langle N\rangle = 4\pi\sigma\rho_0^2\int_0^{R_B^2} d\ b^2(R_B^2-b^2)^{1/2}(R_A^2-b^2)^{1/2} = \tfrac{3}{4}B\sigma\rho_0 R_A\left[1+x^2-\frac{1}{2x}(x^2-1)^2\ln\left(\frac{x+1}{x-1}\right)\right], \quad (42)$$

with $x=R_A/R_B$. From (38) we have

$$N_{pA}=\langle N\rangle^{-1}\sigma^2\int d^2s T_B(s)T_A^2(s) = 8\langle N\rangle^{-1}\sigma^2\pi\rho_0^3\int_0^{R_B^2} d\ b^2(R_B^2-b^2)^{1/2}(R_A^2-b^2) = 4\langle N\rangle^{-1}\sigma^2 B\rho_0^2 R_A^2(1-\tfrac{2}{5}x^2), \quad (43)$$

and from (39),

$$N_{pB}=\langle N\rangle^{-1}\sigma^2\int d^2s T_B^2(s)T_A(s) = 8\langle N\rangle^{-1}\sigma^2\pi\rho_0^3\int_0^{R_B^2} d\ b^2(R_B^2-b^2)(R_A^2-b^2)^{1/2} = 4\langle N\rangle^{-1}\sigma^2 B\rho_0^2 R_B^2(x^3-\tfrac{2}{5}[x^5-(x^2-1)^{5/2}]). \quad (44)$$

For small targets, the assumption $R_B\ll R_A$ used in deriving (40) and (41) overestimates N_{pA} and N_{pB}, as well as the fluctuations. For $B=A$, and $\mathbf{b}=0$, the above results give

$$N_{pA}=N_{pB}=\tfrac{8}{5}\sigma\rho_0 R_A. \quad (45)$$

A diffuse nuclear surface decreases the average density, as well as decreases N_{pA} and N_{pB} from the values calculated above. A numerical calculation with a Woods-Saxon density distribution $\rho=\rho_0/[1+\exp(r-R)/\delta]$, where R is determined from the total number of nucleons in the nucleus and the surface diffuseness is chosen as $\delta=0.55$, yields a further reduction of N_{pA} and N_{pB} of order 20% for $A=28$ to 10% for heavy nuclei, compared to the above results for a sharp surface. The effects are largest for small nuclei, where the nuclear surface is relatively large.

The nuclear gas result (37) is considerably larger than that of the strongly correlated nuclear liquid, Eq. (35), as can be seen in Fig. 3. The discrepancy can be traced back to the differences in the correlation functions. The derivation of (35) assumed that $\xi\ll R_B\ll R_A$, whereas in (37) we took the correlation function $C_A=1/A$, which implies that ξ is of the size of the nuclear radius. The uncorrelated gas result for ω *cannot* be obtained from (35) in the nucleus-nucleus case by choosing appropriate α and β, e.g., as the value $\alpha=\langle N\rangle/A$ in the proton-nucleus case, (14). The larger ω_N in the ideal gas case arises mainly from the second term in Eq. (36). The extra fluctuations are caused by "geometric correlations," that is, if one of the projectile nucleons collides with very few, or with numerous, target nucleons, then there is high probability that the other projectile nucleons will do the same since the projectile nucleons are nearby spatially. Correlations in nuclei, however, reduce the fluctuations in the number of proton-nucleus collisions and effectively cancel the geometric correlations.

[5]The assumption $\xi\ll R_B$ is of course not valid for small projectile nuclei; in the limit $B\to 1$, the term (32) vanishes, and (35) reduces to the result for proton-nucleus collisions, Eq. (10).

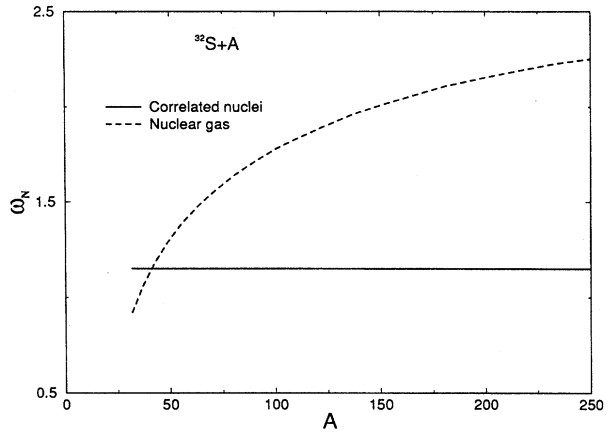

FIG. 3. Fluctuations ω_N for central collisions of ^{32}S on different targets for a strongly correlated nucleus, Eq. (50) (solid line), as well as for a nuclear gas, Eq. (37) (dashed line).

This exercise clearly shows the necessity of treating nuclear correlations carefully in numerical simulations of relativistic heavy-ion collisions. In simulations the nucleons are often positioned successively in the nuclei by Monte Carlo methods with the restriction that they should be at least a distance $\tilde{\xi}$ apart. Such a procedure, as discussed above, describes a free gas with excluded volume, and fails to generate the correlations characteristic of a self-bound liquid. Generally, the correlation function resulting from this procedure has a correlation hole of radius $\tilde{\xi}$, but has a tail which oscillates for large distances and can be negative. While the correlation length, the range of the correlation hole, is close to the interparticle spacing in nuclear matter, $\xi \simeq r_0$, the minimum separation distance of the centers cannot be directly translated into a correlation length. When $\tilde{\xi} > r_0$, the integral of the density over the excluded volume exceeds unity, and the sum rule (6) requires the correlation function to be negative on average outside the excluded volume. (Note that the maximum value of $\tilde{\xi}$ is $\lesssim 2r_0$ in order to accomodate all the nucleons in the nucleus). When $\tilde{\xi} < r_0$ the correlation function has a long tail characteristic of an interacting nuclear gas similar to the "excluded volume" correlation function of Fig. 2.

For example, the Fritiof model requires the centers to be at least 1.13 fm apart [20]. Numerically, this results in $\alpha \simeq 0.4$, and so for proton-nucleus collisions the fluctuations agree with those for the more-correct correlation function. However, in nucleus-nucleus collisions this failure to include liquidlike correlations generally overestimates the fluctuations, as Eq. (37) illustrates. In the Fritiof model one finds, for example, that $\omega_N \simeq 1.77$ in the case of ^{16}O+Au [20], a value between that of a free gas, Eq. (37), and that for a nuclear liquid, Eq. (35). The fact that a simulation reproduces large fluctuations does not imply that it correctly includes the physics producing the fluctuations.

The density distribution resulting from positioning the nucleons by Monte Carlo with a minimum separation can also have the unpleasant feature that it is largest near the nuclear surface. This is because the imposition of a minimum distance between nucleons makes it harder to fit subsequent nucleons into the nucleus; it is easier to accommodate the last ones near the surface where there are fewer neighbors.

A physically correct description of the initial nuclei should not only produce the correct density distribution, but also describe nucleon-nucleon correlations correctly, guaranteeing that the correlation function is generally short ranged, vanishing within a distance less than the nuclear radius, and does not become negative. To implement correlations correctly in numerical Monte Carlo codes requires constructing the initial nuclei by distributing all the particles in a nucleus at a time, rather than attempting to simulate correlations according to a rule that puts the particles in sequentially. The correct probability distribution for the nucleon positions is $|\Psi_A(r_1, r_2, \ldots r_A)|^2$, where Ψ_A is the A-particle ground state nuclear wave function. In practice, for given $|\Psi_A|^2$, one can follow a standard Metropolis algorithm to generate most-probable configurations. Many-body wave functions of Jastrow form, represented as the product of the mean-field wave function and two-nucleon correlators, readily lend themselves to development of generators of initial conditions for collision simulations.[6]

IV. COLOR OPACITY AND TRANSPARENCY, AND CROSS-SECTION FLUCTUATIONS

In hadron-nucleus collisions at high energies, the internal configuration of the color-carrying degrees of freedom of the projectile hadron are frozen by Lorentz time dilation [21,22]. The hadron-nucleon cross section is, as a consequence, characterized by a probability distribution $P(\sigma)$. The condition for a projectile nucleon to be frozen in passing through a target nucleus is that the crossing time $2R_A/c$ be less than the internal dynamic time, given by the uncertainty relation between time and energy [23],

$$2R_A \lesssim \frac{1}{\Delta E} \simeq \frac{2p_{lab}}{m_{N*}^2 - m_N^2} \simeq \frac{\gamma}{m_{N*} - m_N}, \qquad (46)$$

where m_N is the nucleon mass, N^* is the lowest-lying resonance with the quantum numbers of the nucleon, of mass $m_{N*} \simeq 1.5$ GeV, and γ is the Lorentz factor. This condition is well-satisfied for projectile energies above $p_{\rm lab} \gtrsim 40$ GeV/c for heavy nuclei, as at the CERN SPS and LHC, and RHIC. The concept of cross-section fluctuations is well established in inelastic shadowing and diffractive hadron-hadron scattering, as well as in coherent diffractive-dissociation of hadrons scattering on nuclei, and is an essential feature of the dynamics of ultrarelativistic heavy-ion collisions [6,14].

The effects of cross-section fluctuations are multifold. When a hadron is in a "small-sized configuration" its inter-

[6]In particular, S. Pieper (private communication) of Argonne National Laboratory has generated useful simplified approximations to many-body nuclear wave functions ([18] and unpublished) of the Jastrow form that correctly reproduce the A-particle spatial distribution functions, although not the details of the spin correlations. These wave functions have recently been employed by Seki *et al.* [19] to study correlation effects in nuclear transparency in $(e,e'p)$ in heavy nuclei.

actions are suppressed because of the small spatial extent of the color fields in the hadron, which leads to the phenomenon of color transparency [24]. On the other hand, a hadron in a frozen "large hadronic configuration" experiences a stronger interaction characterized by a cross section $\sigma > \bar{\sigma}$, its average value, when passing through a nucleus, a "color opacity" effect. We now discuss, in further detail than in Ref. [6], and also for the more general case where the projectile B is not necessarily much smaller than the target A, how these effects lead to enhancement of the fluctuations in observables such as transverse energy and multiplicity. We then compare with fluctuations found at CERN.

In calculating average quantities such as the mean number of collisions $\langle N \rangle$ the cross section σ can be replaced by its average value $\bar{\sigma} = \langle \sigma \rangle_I \simeq 32$ mb, where the subscript I refers to the average over internal configurations. However, in calculating fluctuations, one must first calculate for a given internal configuration and then average the final result. In particular the average of the square of the cross section for collisions of the projectile p with successive target nucleons j and j' is given by[7]

$$\langle \sigma_{pj} \sigma_{pj'} \rangle_I \equiv \bar{\sigma}^2 (1 + \omega_\sigma) , \tag{47}$$

and the scaled variance of the cross-section fluctuations, ω_σ, is given by

$$\omega_\sigma \equiv \frac{\langle \sigma^2 \rangle_I}{\bar{\sigma}^2} - 1. \tag{48}$$

The freezing of the projectile configuration during the passage across the nucleus correlates σ_{pj} and $\sigma_{pj'}$ through the internal coordinates of the projectile. When the projectile is in a small configuration it has a small probability to scatter on *both* j and j', and when in a large configuration is has a large probability to do so. [On the other hand, a slow projectile has ample time to change its internal structure between collisions; subsequent collisions are uncorrelated and then $\langle \sigma_{pj} \sigma_{pj'} \rangle_I = \bar{\sigma}^2$, so that $\omega_\sigma = 0$.] As we showed in Refs. [6,7,14,15,25], the size and form of the cross-section fluctuations can be extracted from diffractive scattering experiments.

Fluctuations of the color degrees of freedom of a hadron lead to fluctuations in the overall scale as well as shape and range of its interaction cross-section $d\sigma/d^2b$ with other hadrons. In the following we shall assume for simplicity that only the scale σ of the cross-section fluctuates but not its shape or range r_σ [see, e.g., Eq. (24)]. Fluctuations in shape and range can lead to further corrections to the effects we found from including the finite interaction range, which should be modeled in the future. Employing the parametrization (24), we see that σ^2 enters as a common prefactor in (7); inclusion of cross-section fluctuations at this level thus simply multiplies the right side of (7) by a factor $1 + \omega_\sigma$, and we directly obtain the scaled variance in proton-nucleus collisions,

$$\omega_N = 1 - \alpha + \omega_\sigma (\langle N \rangle - \alpha). \tag{49}$$

The important new ingredient is the last term due to the fluctuations in cross sections. For a central p-^{208}Pb collision, $\langle N \rangle \simeq 7$, and with $\omega_\sigma \sim 0.2$–0.3 at high energies as estimated in Ref. [14], cross-section fluctuations contribute ~ 1.5–2.0 to ω_N, thus increasing ω_N by a factor 2–3.

The fluctuations in nuclear collisions can be calculated analogously to the proton-nucleus case. In the four terms of Eq. (29), only the second and third involve multiple collisions of the same nucleon; therefore, in these terms we must replace the prefactor σ^2 by $\bar{\sigma}^2(1 + \omega_\sigma)$. The fluctuations in the number of NN collisions in central nucleus-nucleus collisions for $\xi < R_B$ are thus given by

$$\omega_N = 1 + \gamma - \alpha - \beta + \omega_\sigma (N_{pA} + N_{pB} - \alpha - \beta) . \tag{50}$$

We can interpret the ω_σ term as the correlation coming from each projectile nucleon making on average $N_{pA} - \alpha$ hits in the target, and a target nucleon being hit on average $N_{pB} - \beta$ subsequent times by projectile nucleons. Equation (50) generalizes the proton-nucleus result of Eq. (49) to nuclear collisions by adding the correlations from target nucleons being hit multiple times. Expressions for N_{pA} and N_{pB} are given in the preceding section, Eqs. (38)–(45).

V. TRANSVERSE ENERGY SPECTRA

We show in this section the importance of correlations and cross-section fluctuations by calculating their contribution to the fluctuations observed in transverse energy spectra in ultrarelativistic heavy-ion collisions, e.g., by NA34 [4]. Different microscopic models of nucleus-nucleus collisions use either the number of binary NN collisions or the number of participating nucleons for the sources of particle or E_T production [26]. We first discuss the fluctuations in a binary collision picture, and then turn to the participant, or "wounded," nucleon picture.

A. Fluctuations in binary collisions

In an independent-source description of collisions, the E_T distribution is obtained by folding the E_T contributions from N sources, where the distribution of the number of sources has mean $\langle N \rangle$. The overall form of the transverse energy distribution in a high-energy nucleus-nucleus collision is determined by the geometry of the collision, as is well-illustrated in the NA34 geometric model, where the E_T distribution is obtained by folding the E_T contribution from N sources (which becomes Gaussian distributed for sufficiently large N), multiplying by the distribution of sources $d\sigma/dN$, and summing over N:

$$\frac{d\sigma}{dE_T} = \int dN \, \frac{d\sigma}{dN} \, \frac{e^{-(E_T - N\epsilon_0)^2/2\omega N \epsilon_0^2}}{(2\pi\omega N \epsilon_0^2)^{1/2}} . \tag{51}$$

The parameter ϵ_0 is interpreted in the NA34 model as the average E_T produced per source, while ω describes the stan-

[7] We assume that the internal degrees of freedom decouple from the nuclear wave function coordinates, i.e., we neglect small modifications of the properties of nucleons in nuclei as revealed by the EMC effect. We also do not distinguish here the dispersion of the inelastic and total cross sections, since they are very close.

dard deviation or fluctuation around the mean value; both parameters are extracted by fitting to data. We do not take this interpretation literally here, but rather adopt the point of view that the model provides a useful parametrization of the data.

The cross section for making N sources, which is taken to be the number of binary collisions, is

$$\frac{d\sigma}{dN}=\int d^2b P_N(b), \tag{52}$$

where $P_N(b)$ is the probability for making N sources in a collision at impact parameter b. In the simplest geometric model, P_N is nonzero only at the mean number of sources, $\bar{N}(b)$, for given impact parameter; for example, for small projectiles B and spherical target nuclei of radius R_A, one has $\bar{N}(b)=2B\bar{\sigma}\rho_0(R_A^2-b^2)^{1/2}$. More generally one can take $P_N(b)$ to be a Poisson distribution around the mean, but, as we have discussed above, correlations lead in fact to a much narrower structure for P_N than Poisson. Equation (51) also describes the multiplicity distribution when E_T is replaced by the multiplicity n; the parameter ϵ_0 is then replaced by the average number of particles produced per source, and ω becomes the corresponding scaled variance.

Our calculations above for the fluctuations in collision numbers are for given impact parameter b; averaging over impact parameters broadens the spectra and increases the fluctuations. The effect of impact parameter averaging is in fact separated out in the NA34 analyses of nucleus-nucleus collisions [4]. As described in Ref. [27], the tail of the E_T distribution in ultrarelativistic heavy-ion collisions is determined by central events, on which we concentrate here.[8] The NA34 analysis thus provides a reliable, albeit model-dependent, way to extract the fluctuations ω for central ($b=0$) collisions from data, and yields values of ω in collisions of ^{32}S on nuclear targets which range, in the pseudorapidity interval $-0.1<\eta<2.9$, from $\sim$ 1.5 to $\sim$ 5.8. The ω's extracted from the NA34 analyses directly describe the transverse-energy fluctuations in central collisions,

$$\omega\equiv\langle N\rangle\frac{\langle E_T^2\rangle-\langle E_T\rangle^2}{\langle E_T\rangle^2}, \tag{53}$$

where $\langle N\rangle$ is evaluated at zero impact parameter. The problem is to understand the physics producing the large values of ω needed by NA34. As we first discussed in Ref. [6], and expand on here, cross-section fluctuations lead to a substantial contribution to ω, capable of explaining deviations of standard estimates from experiment [4,5].

The principal contributions to ω are

$$\omega=\omega_0+\omega_{\rm def}+\omega_N, \tag{54}$$

where ω_0 is the width of the single source E_T distribution, $\omega_{\rm def}=4\langle N\rangle\delta^2/45$ is the variance of the fluctuations from the deformation of the target, with δ the nuclear deformation parameter, particularly large for W and U. The third term, $\omega_N=(\langle N^2\rangle-\langle N\rangle^2)/\langle N\rangle$, takes into account fluctuations in the number of sources in a central collision. With the assumption that the number of sources is given by the number of binary collisions, fluctuations in the number of sources is given by Eq. (35) in the absence of cross-section fluctuations, and Eq. (50) with cross-section fluctuations included.[9]

Using $\omega_0\approx 0.5$ as determined from pp collisions in the comparable energy and rapidity range, one cannot, with these assumptions in the absence of cross-section fluctuations, explain the experimentally observed large fluctuations.[10] With $\bar{\sigma}\simeq 32$ mb and $\rho_0\simeq 0.15$ fm^{-3}, and a heavy target we have $N_{pA}\simeq 2\bar{\sigma}\rho_0 R_A\simeq 1.2A^{1/3}$. In CERN and Brookhaven experiments, with ^{16}O or ^{32}S projectiles, $N_{pB}\simeq\frac{3}{2}\bar{\sigma}\rho_0 R_B\simeq 2-3$. We show in Fig. 4 $\omega-\omega_{\rm def}=\omega_N+\omega_0$ given by Eq. (50), for ^{32}S, with various values of ω_σ, taking $\omega_0=0.5$, $\alpha=\beta=0.25$, and $\gamma=0.15$, as discussed above. We see that cross-section fluctuations are able to account for the large ω's found experimentally with $\omega_\sigma\sim 0.25$, a value consistent with that extracted from inelastic shadowing in nucleon-deuteron scattering as well as forward diffractive scattering amplitudes at CERN-SPS energies [14]. Equation (50) describes the ^{16}O data [30] as well with similar values for ω_σ. To disentangle the color transparency and opacity effects from other sources of E_T fluctuations in future experiments, especially rescattering, it will be useful to study the energy and rapidity dependence of the E_T fluctuations. To go beyond the variance ω and calculate the full E_T spectra requires building a detailed model for AA collisions that includes color fluctuations as well as nuclear correlations. Outlines of how to construct such a model are discussed in the Sec. III and in the Conclusion. We hope to move in this direction in the near future.

[8]The procedure of extracting fluctuations at given impact parameter is much more difficult for proton-nucleus collisions which do not exhibit the plateau spectrum in nucleus-nucleus collisions. While the characteristic "shoulder" in nucleus-nucleus E_T spectra marks the beginning of a region dominated by central collisions, in proton-nucleus collisions impact-parameter averaging results in a long tail which is further smeared by fluctuations as well as degradation and rescattering [28].

[9]The experimentally extracted values of ω include a small contribution $\omega_{\rm res}$ from the finite energy resolution of the detectors, $\Delta E/\langle E\rangle\sim 0.45/\sqrt{E_{\rm GeV}}$ (where $E_{\rm GeV}$ is the energy in units of GeV), which leads to $\omega_{\rm res}=(0.45)^2\langle N\rangle/E_{\rm GeV}$ of order 0.2; we are grateful to H. Ströbele for emphasizing the existence of this contribution. In Eq. (54) we also have neglected terms due to decrease of the transverse-energy production per source in successive hits. As argued in Ref. [5] these terms lead to a small reduction of ω.

[10]Rescattering of secondaries might be expected to broaden the tails of the E_T distribution and thus increase ω, since it allows a secondary to lead to a wider range of transverse energy and multiplicity in final states. But rescattering also increases the number of scatterings and thus tends to narrow the fluctuations; in general, adding more degrees of freedom to a system while keeping its average output fixed decreases its fluctuations. A calculation for central collisions of ^{32}S on Au at CERN-SPS energies by Werner [29] using the VENUS 4.16 code both with and without rescattering shows no significant change in the relative width of the distribution. We are indebted to K. Werner for providing us with the results of this calculation.

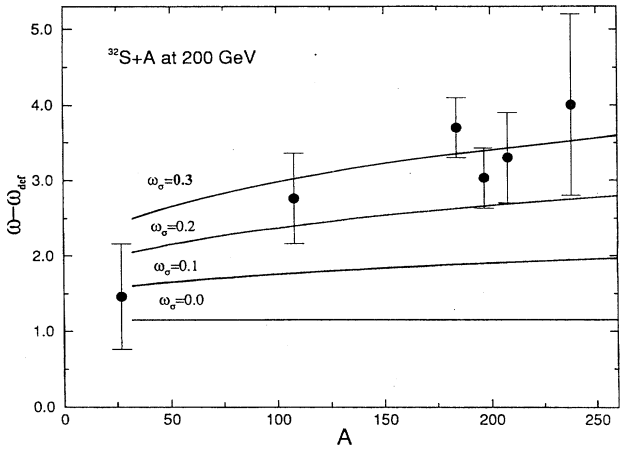

FIG. 4. Fluctuations $\omega-\omega_{\rm def}=\omega_0+\omega_N$ for central collisions of ^{32}S on different targets for $\omega_\sigma=0.0$, 0.1, 0.2, and 0.3 calculated with Eq. (50). The experimental values (dots) are taken from Ref. [4].

B. Fluctuations in participants or "wounded nucleons"

Let us consider briefly the fluctuations in a model in which the number of sources is the number of participant or wounded nucleons. The number of sources in proton-nucleus collisions is very similar for the binary-collision and the wounded-nucleon pictures, since the number of participants is just the number of binary collisions plus one, the projectile. Similarly, the fluctuation around the mean number of sources is almost the same. For nuclear collisions the numbers of sources in the two pictures can differ considerably [11].

The geometric-model result (51) can also be applied in the wounded-nucleon picture. The interpretation of the source parameters ϵ_0 and ω_0 is, however, very different in the two pictures. In the binary collision model ϵ_0 is the transverse energy produced in a nucleon-nucleon collision whereas in the wounded nucleon model it is half that value. As we see from Eq. (53), $\Omega\equiv\omega/\langle N\rangle$ is the same in both cases.

The number of participants in a nucleus-nucleus collision is given by

$$\langle N\rangle_{\rm WN}\simeq\int d^2s[T_B(\mathbf{s})(1-e^{-\sigma T_A(\mathbf{s}+\mathbf{b})}) + T_A(\mathbf{s}+\mathbf{b})(1-e^{-\sigma T_B(\mathbf{s})})], \quad (55)$$

a formula which assumes $\sigma\ll\pi R_B^2$. When the projectile is much smaller than the target nucleus this result simplifies to

$$\langle N\rangle_{\rm WN}\simeq B(1-e^{-N_{pA}})+\pi R_B^2 T_A(b)\left(1-\frac{2}{\tilde N_{pB}^2}\times[1-(1+\tilde N_{pB})e^{-\tilde N_{pB}}]\right), \quad (56)$$

where $N_{pA}=\sigma T_A(b)$ and $\tilde N_{pB}=\sigma T_B(0)$. While N_{pA} is the same as in Eq. (38), $\tilde N_{pB}$ is a factor 3/4 smaller than N_{pB} in Eq. (39).

In the limit in which all nucleons in the overlapping volume of the two nuclei in the collision participate, i.e., small nucleon mean free-paths, corresponding to large N_{pA} and $\tilde N_{pB}$, and assuming sharp nuclear surfaces we find from (55) that for central collisions

$$\langle N\rangle_{\rm WN}=B+A-|A^{2/3}-B^{2/3}|^{3/2}. \quad (57)$$

For small projectiles (57) reduces to

$$\langle N\rangle_{\rm WN}\simeq B+\pi R_B^2 T_A(b)\ , \quad B\ll A\ , \quad (58)$$

valid in this form also for noncentral impact parameters. In comparison, the mean number of binary collisions, $\langle N\rangle\simeq B\sigma T_A(b)$, is generally is larger.

The latter results are, to first approximation, independent of the cross section; therefore we do not expect fluctuations in σ_{ij} in this limit to affect the distribution of wounded nucleons significantly.

To estimate the fluctuations in the number of participants including correlations, we limit ourselves for simplicity to central collisions and assume sharp nuclear surfaces and the limit of short nucleon mean free paths. In this limit, with $B\leqslant A$, all nucleons from nucleus B participate and so there are no fluctuations in that number. The fluctuation in the number of participants in nucleus A is determined from

$$\langle N(N-1)\rangle_{{\rm WN}\in A}=\int d^3r d^3r'\ \rho_A^{(2)}(\mathbf{r},\mathbf{r}')\,\theta(R_B-|\mathbf{r}_\perp|)\times\theta(R_B-|\mathbf{r}'_\perp|)\ . \quad (59)$$

[Note the formal similarity of this equation to Eq. (4) for pA collisions with the range r_s of the nucleon-nucleon interaction replaced by R_B.] For an uncorrelated nuclear gas, for which $\xi=R_A$ and $C_2=1/A$, Eq. (59) gives $=\langle N\rangle^2_{{\rm WN}\in A}(1-1/A)$ and so $\omega_N=1-\langle N\rangle/A$, the usual binomial result [cf. (14)]. More realistically, $\xi\ll R_B$, in which case Eq. (59) implies $\langle N^2\rangle_{{\rm WN}\in A}=\langle N\rangle^2_{{\rm WN}\in A}$ and thus $\omega_N=0$ [cf. (18)]. Correlations effectively eliminate fluctuations in $N_{\rm WN}$. Fluctuations in observables arise only from fluctuations in the individual sources, given by $\omega_{0,{\rm WN}}=2\omega_0$, since two wounded nucleons make up one binary NN collision. To compare the predictions of fluctuations in the wounded-nucleon picture to the NA34 data, we should keep in mind the conventional but arbitrary scaling by $\langle N\rangle$ in the relation of (53) to the fluctuations in transverse energy, and thus compare $\omega_{\rm WN}=2\omega_{0,{\rm WN}}\langle N\rangle/\langle N\rangle_{\rm WN}\simeq 1-2$ to the ω extracted in the NA34 geometric model. The fluctuations in the wounded-nucleon picture are generally not large enough to explain the NA34 data.

VI. CONCLUSION

As we have seen, nucleon correlations in projectile and target nuclei, the range of the underlying NN interactions, and cross-section fluctuations are all important for determining fluctuations in the number of NN collisions and thus observables in nuclear collisions. Correlations reduce the density fluctuations and therefore also the fluctuations in the number of NN collisions. Because the nucleus is a self-bound liquid of nucleons, correlations are particularly impor-

tant in nucleus-nucleus collisions, and lead to significant reduction in fluctuations compared to those for a gas of nucleons assumed freely swarming in the nucleus. Interestingly, the correlations in the incident nuclei are one of the few features of the original nuclear structure that are a determining factor in high-energy collisions. Allowing for a larger range for the interaction or collision probability reduces the effect of the correlations between two nearby nucleons, and increases the fluctuations. Cross-section fluctuations are an important feature of collisions of a hadronic projectile at sufficiently high energy that time dilation does not allow the projectile to change its configuration between successive collisions in the target nucleus. In this case successive collisions become correlated, with the effect of increasing the fluctuations in the number of NN collisions significantly.

We emphasize the need to incorporate the physics we discussed here into Monte Carlo event generators for AA collisions. The method currently applied in many Monte Carlo codes of constructing initial conditions by successively filling a nucleus with nucleons separated by a minimum distance does not reproduce nuclear correlations and fluctuations satisfactorily, especially in nucleus-nucleus collisions; approaches to implementing nuclear correlations that correctly describe a nuclear liquid were discussed at the end of Sec. III. To a first approximation, cross-section fluctuations can be incorporated in the probabilistic language of Sec. III by assuming factorization for interactions of two nucleons (1 and 2) in different configurations, i.e., assuming the cross section to have the form, $\sigma=\sigma_1\sigma_2/\bar{\sigma}$ (cf. discussion in [6,7]), and then generating σ for each of the nucleons with individual weights $P(\sigma_1)$ and $P(\sigma_2)$, where $P(\sigma)$ is the normalized distribution of cross sections for NN scattering [14].

Beyond fluctuations in the probability of collisions, one should also incorporate fluctuations in the outcomes of individual collisions, i.e., fluctuations on the parton level. Since parton distributions depend on the size of the nucleon configuration, fluctuations in internal nucleon configurations lead directly to fluctuations in parton distributions and hard parton-parton interactions. While microscopic collision models in terms of partons have been developed for ultrarelativistic heavy-ion collisions (see, e.g. [31,32]), they so far only take fluctuations in number of collision partners into account, employing average structure functions, or parton momentum distribution functions, for individual nucleons. A simple way to take fluctuations on the parton level in account in such models, based on the fact that increase of the effective transverse size of a hadron allows emission of softer partons, is to let the parton distributions $p_N(x,Q^2,\sigma)$ scale as

$$p_N(x,Q^2,\sigma)=p_N(x,Q^2\sigma/\bar{\sigma}), \tag{60}$$

similar to the rescaling model of the EMC effect [33].

At small x one also has to take into account shadowing and enhancement effects which depend both on σ and the impact parameter of the colliding nucleon [13]; discussion of these effects is beyond the scope of this paper. Furthermore, observed fluctuations in hard parton-parton interactions will depend on the subset of events on which one triggers in a collision (see [34] and discussion in [25]), e.g., biasing towards high E_T events will enhance the probability of large interaction cross-section configurations occurring in the colliding nuclei. Methods to study this phenomenon experimentally in pA collisions are discussed in [35].

ACKNOWLEDGMENTS

This work was supported by NSF Grants Nos. PHY 89-21025 and PHY 94-21309, DOE Contract No. DE-AC03-76SF00098, DOE Grant No. DE-FG02-93ER40771, and Binational Scientific Foundation (BSF) Grant No. 9200126. B.B. is grateful for support from the Alexander von Humboldt Stiftung and H.H. from the Danish Natural Science Research Council. We thank Steven Pieper, Vijay Pandharipande, Heinz Sorge, and Evert Stenlund for useful discussions.

APPENDIX A: THE AGK CUTTING RULES AND BINARY COLLISIONS

The AGK diagram cutting rules for high-energy scattering processes [8,9] lead to the theorem that in nucleon-nucleus (NA) scattering, inclusive particle production away from the projectile fragmentation region is simply that in NN scattering times the number of nucleons, A, in the target nucleus. In this Appendix we briefly discuss the extension of this result to nucleus-nucleus collisions at central rapidities, to give an indication of how the probabilistic methods we have used in this paper can be extracted from a more formal field-theoretic approach. The prediction of the theorem for nucleus-nucleus collisions that particle production scales with the number of NN collisions supports the use in this paper of the binary collision model in describing fluctuations in the central rapidity range.

The theorem is based on the Glauber multiple NN scattering formalism within the eikonal approximation, and thus ignores rescattering of produced particles during the collision. Rescattering of target nucleons on other target nucleons is not taken into account, and in nucleus-nucleus collisions neither is scattering of projectile nucleons on other projectile nucleons. In addition, coherent processes, such as showers of particles overlapping spatially and interacting strongly, are ignored, as is a possible transition to a quark-gluon plasma in which particle production cannot be described in terms of nucleon-nucleon interactions. Finally, the AGK theorem ignores constraints from global energy conservation in multiple NN collisions, and is thus valid only at those rapidities and at sufficiently large energies that particle production depends slowly on the initial energy. Within these assumptions, AGK show that there is an exact cancellation of processes involving inelastic interactions of the projectile with more than one nucleon at a time. For example, in the interaction of the projectile with two nucleons, the forward amplitudes for the two processes where the projectile interacts inelastically with one of the nucleons and elastically with the other cancels against the amplitude for production of particles in inelastic interactions with both nucleons. The net result is that the total multiplicity in inelastic collisions is the sum of the

multiplicities in inelastic collisions of the projectile with individual nucleons.

In the projectile fragmentation region in NA scattering, global energy conservation constrains particle production; the cancellation fails in the projectile fragmentation region because the way in which the projectile energy is shared in inelastic collisions depends on the number of target nucleons with which it collides. The net result is shadowing of particle production close to the projectile rapidity.[11] The more nucleons involved in a collision, the stronger is the constraint of global energy conservation, and the wider the rapidity interval where the AGK cancellation is not effective. For example, in central nucleus-nucleus collisions at lab energy of 200 GeV/A, as at CERN, the limited total energy constrains particle production in the nuclear fragmentation regions, and precludes application of the AGK theorem there.

The extension of the AGK theorem to nucleus-nucleus (BA) collisions, for particle production away from nuclear fragmentation regions, is:

$$\sigma^{BA\to a+X}=BA\,\sigma^{NN\to a+X}\,, \tag{A1}$$

where $\sigma^{BA\to a+X}$ and $\sigma^{NN\to a+X}$ are the inclusive cross sections for producing particle a in BA and NN collisions respectively. The number of particles a produced per collision is

$$\nu^{BA\to a}=\frac{\sigma^{BA\to a+X}}{\sigma^{BA}}\,, \tag{A2}$$

where σ^{BA} is the total production cross section for colliding nuclei A and B (i.e., not including quasielastic processes in which no hadrons are produced); for NN scattering $\sigma^{NN}=\bar{\sigma}$. The mean number of NN collisions averaged over impact parameter is then

$$\langle N\rangle=\frac{\nu^{BA\to a}}{\nu^{NN\to a}}=BA\,\frac{\sigma^{NN}}{\sigma^{BA}}\,, \tag{A3}$$

a result in fact independent of the particle a. By writing this equation as

$$\langle N\rangle=\int\frac{d^2b}{\sigma^{BA}}\,\sigma^{NN}\int d^2s\,T_A(\mathbf{s}+\mathbf{b})T_B(s), \tag{A4}$$

we may interpret Eq. (63) as an average of impact parameter of the number of collisions at given impact parameter,

$$\langle N(b)\rangle=\sigma^{NN}\int d^2s\,T_A(\mathbf{s}+\mathbf{b})T_B(s). \tag{A5}$$

[11]One can, in fact, extend the AGK arguments to include energy conservation within the Glauber model, and derive descriptions of the bulk characteristics of hadron-nucleus scattering in good agreement with available data ($E_{\rm inc}\lesssim 400$ GeV) [reviewed in [36]].

[Cf. Eq. (27)]. The generalization of Eq. (A4) to a finite interaction range is outlined and applied to diffractive scattering and inelastic shadowing effects in Refs. [37,7,14].

The above example indicates the correspondence between the probabilistic language of Sec. III and field theory. The AGK theorem applied to nucleus-nucleus collisions leads to the same partial probabilities as the binary collision model of collisions involving a given number of nucleons in inelastic interactions. Binary collision models make particular assumptions about how energy is shared in the various subcollisions. At central rapidities, where the energy constraints are unimportant, the results are independent of these assumptions, and one can apply the AGK theorem. However, binary collision models give specific predictions in the fragmentation regions as well.

At very high energies the contribution of minijets to particle and E_T production starts to become comparable to that from soft processes. According to *Eskola et al.* [32] minijets contribute more than 50% at energies above RHIC energies, $\sqrt{s}\gtrsim$ 200 GeV (such estimates, however, carry the uncertainty of how low in transverse momentum one can use perturbative qcd to calculate jet production). Since minijets are hard processes with kinematics where nuclear shadowing in the parton distributions can be neglected, they are produced independently in each NN collision. Hence in this case the binary collision model for parton-parton scattering should be valid, although one has to take into account fluctuations in the parton distributions on nucleons; cf. Eq. (60).

The inclusion of color fluctuation effects in the description of nucleus-nucleus collisions for calculation of total cross sections is equivalent in qcd to inclusion of Gribov inelastic shadowing effects, the presence of inelastic intermediate states in the inelastic eikonal approximation (at the level where one neglects the high-mass diffraction, described by *triple Pomeron* diagrams). The use of the eigenstate formalism [38,39] (applied in this context in Refs. [14,25]) allows one to diagonalize the transition matrices in the inelastic eikonal diagrams and write these diagrams as a sum of terms corresponding to the scattering of nucleons in the states with fixed σ. The probabilistic interpretation of the eikonal approximation for the multiple scattering combinatorics is thus preserved even in the presence of color fluctuations, allowing one to understand the results of Sec. III from a field-theoretic perspective. For example, Eq. (29), with color fluctuations, can be derived using the AGK rules for the double inclusive spectrum. Indeed, any quantity calculated in the eikonal approximation proportional to σ^n is given, with color fluctuations taken into account, by the same expression with the substitution $\sigma^n\to\langle\sigma^n\rangle$.

We also note that the AGK cutting rules connect the cross sections for inelastic incoherent hadron production and diffractive hadron production, as arising from different cuts of the same diagrams. Hence coherent hadron diffraction in hadron-nucleus collisions can be calculated using the same distribution of cross sections $P(\sigma)$ [40] as used for inelastic incoherent hadron production. The agreement of the results of the calculation of inelastic coherent diffractive processes in hadron-nucleus scattering with existing data [41] provides a further confirmation of the picture of color fluctuations adopted here.

[1] For WA85, see S. Abatzis *et al.*, Nucl. Phys. **A566**, 491c (1994); Phys. Lett. B **270**, 123 (1991); **259**, 508 (1991).
[2] For NA35, see J. Barke *et al.*, Z. Phys. C **48**, 191 (1990).
[3] For NA38, see M.C. Abreu *et al.*, Nucl. Phys. **A566**, 77c (1994).
[4] For NA34, see J. Schukraft *et al.*, Nucl. Phys. **A498**, 79c (1989).
[5] G. Baym, G. Friedman, and I. Sarcevic, Phys. Lett. B **219**, 205 (1989).
[6] H. Heiselberg, G.A. Baym, B. Blättel, L.L. Frankfurt, and M. Strikman, Phys. Rev. Lett. **67**, 2946 (1991).
[7] B. Blättel, G.A. Baym, L.L. Frankfurt, H. Heiselberg, and M. Strikman, Nucl. Phys. **A544**, 479c (1992).
[8] V.A. Abramovskiĭ, V.N. Gribov, and O.V. Kancheli, Sov. J. Nucl. Phys. **18**, 308 (1974).
[9] L. Bertocchi and D. Trelleani, J. Phys. G **3**, 147 (1977).
[10] J. Whitmore *et al.*, Z. Phys. C **62**, 199 (1994).
[11] EMU01 Collaboration, R.J. Wilkes *et al.*, Nucl. Phys. **A544**, 153c (1992).
[12] L.L. Frankfurt, G.A. Miller, and M. Strikman, Annu. Rev. Nucl. Part. Phys. **44**, 501 (1994).
[13] L.L. Frankfurt, S. Liuti, and M. Strikman, in Proceedings of the Fourth Workshop on Experiments and Detectors for RHIC, BNL Report No. 52262 (unpublished), 1990, p. 103.
[14] B. Blättel, G.A. Baym, L.L. Frankfurt, H. Heiselberg, and M. Strikman, Phys. Rev. D **47**, 2761 (1993).
[15] B. Blättel, G.A. Baym, L.L. Frankfurt, and M. Strikman, Phys. Rev. Lett. **70**, 896 (1993).
[16] H. Miettinen and J. Pumplin, Phys. Rev. D **18**, 1696 (1978).
[17] O. Benhar, A. Fabrocini, S. Fantoni, G.A. Miller, V.R. Pandharipande, and I. Sick, Phys. Rev. C **44**, 2328 (1991).
[18] S. Pieper, in Atomic and Nuclear Physics at One Gigaflop, Nuclear Science Research Conference Series Volume 16, Oak Ridge, April, 1988, edited by C. Bottcher, M.R. Strayer, and J.B. McGrory.
[19] R. Seki, T.D. Shoppa, A. Kohama, and K. Yazaki, Caltech report, 1995.
[20] R. Albrecht *et al.*, Z. Phys. C **45**, 31 (1989).
[21] S. Mandelstam, Nuovo Cimento **30**, 1127, 1148 (1963).
[22] V.N. Gribov, Zh. Éksp. Teor. Fiz. **56**, 483 (1969); Sov. Phys. JETP **30**, 709 (1970).
[23] L.L. Frankfurt and M. Strikman, Phys. Rev. Lett. **66**, 2289 (1991); G.R. Farrar, L.L. Frankfurt, M.I. Strikman, and H. Liu, *ibid.* **61**, 686 (1988).
[24] A.H. Mueller, in *Proceedings of the 17th Rencontre de Moriond*, Les Arc, 1982, edited by J. Tran Thanh Van (Editions Frontières, Paris 1982); S.J. Brodsky, in *Proceedings of the 13th International Symposium on Multiparticle Dynamics*, Volendam, 1982, edited by W. Kittel *et al.* (World Scientific, Singapore, 1983); L.L. Frankfurt, Professor Habilitatus thesis, Leningrad, 1991.
[25] G. Baym, L.L. Frankfurt, and M. Strikman, Nucl. Phys. **A566**, 149c (1994).
[26] G. Baym, P. Braun-Munzinger, and P.V. Ruuskanen, Phys. Lett. **B 190**, 29 (1987); H. Bøggild and A.D. Jackson, Nucl. Phys. **A470**, 669 (1987); M. Prakash, A.D. Jackson and S. Das Gupta, *ibid.* **A489**, 716 (1988).
[27] G. Baym, G. Friedman, and H. Heiselberg, Proceedings of the Brookhaven HIPAGS Workshop, March, 1990, edited by O. Hansen (unpublished).
[28] H. Heiselberg, Phys. Scr. **40**, 587 (1989).
[29] K. Werner and P. Koch, Phys. Lett. B **242**, 251 (1990).
[30] Helios Collaboration, T. Åkesson *et al.*, Z. Phys. C **38**, 383 (1988).
[31] K. Kinder-Geiger and B. Mueller, Nucl. Phys. **B369**, 600 (1992); K. Geiger, Phys. Rev. D **47**, 133 (1993); K. Geiger, Phys. Rep. (in press) (Report No. CERN-TH 7313/94).
[32] K.J. Eskola, K. Kajantie, and J. Lindfors, Nucl. Phys. **B323**, 37 (1989); K. J. Eskola, K. Kajantie and P. V. Ruuskanen, Phys. Lett. B **332**, 191 (1994); K.J. Eskola and X. N. Wang, Phys. Rev. D **49**, 1284 (1994).
[33] F.E. Close, R.G. Roberts, and G.G. Ross, Phys. Lett. **134B**, 449 (1984).
[34] A. Bulgac and L. Frankfurt, Phys. Rev. D **48**, R1894 (1993).
[35] L.L. Frankfurt and M. Strikman, Nucl. Phys. **B250**, 147 (1985).
[36] V.M. Braun and Yu.M. Shabelskii, Int. J. Mod. Phys. **A3**, 2417 (1988).
[37] V.N. Gribov, Zh. Éksp. Teor. Fiz **53**, 654 (1967) [Sov. Phys. – JETP **26**, 414 (1968)].
[38] E.L. Feinberg and I.Y. Pomeranchuk, Suppl. Nuovo Cimento **III**, 652 (1956).
[39] M.L. Good and W.D. Walker, Phys. Rev. **120**, 1857 (1960).
[40] L. Frankfurt, G.A. Miller, and M. Strikman, Phys. Rev. Lett. **71**, 2859 (1993).
[41] W. Mollet *et al.*, Phys. Rev. Lett. **26**, 1646 (1977); M. Zielinski *et al.*, Z. Phys. C **16**, 197 (1983).